ELSEVIER

Journal of Physics and Chemistry of Solids 64 (2003) 665–676

JOURNAL OF PHYSICS AND CHEMISTRY OF SOLIDS

www.elsevier.com/locate/jpcs

Translational and rotational mode coupling in disordered ferroelectric $KTa_{1-x}Nb_xO_3$ studied by Raman spectroscopy

Oleksiy Svitelskiy*,[1], Jean Toulouse

Department of Physics, Lehigh University, Bethlehem, PA 18015, USA

Received 10 April 2002; revised 1 July 2002; accepted 1 August 2002

Abstract

The coupling of translational modes to the reorientational motion is an essential property of systems with internal orientational degrees of freedom. Due to their high complexity most of those systems (molecular crystals, glasses, etc.) present a major puzzle for scientists. In this paper we analyze the Raman scattering of a relatively simple ferroelectric system, $KTa_{1-x}Nb_xO_3$, which may serve as a model for more complicated cases. We show the presence of a strong coupling between translational and reorientational motion in the crystal. Our data suggest that this coupling is the main reason for the depolarized component of the second-order Raman spectra and that it is also responsible for the frequency decrease (softening) of the transverse acoustic mode down to the third of three transitions, below which reorientational motion is no longer allowed.

PACS: 77.84.Dy; 77.80. − e; 63.20.Mt; 78.30. − j

Keywords: D. Ferroelectricity; D. Lattice dynamics; C. Raman spectroscopy

1. Introduction

Much of the recent ferroelectric research has been focused on the new and industrially promising lead-based relaxor materials. Unfortunately, from a basic point of view, these materials are highly complex, presenting both chemical and structural local order, such as in $PbMg_{1/3}Nb_{2/3}O_3$ [1] or $PbZn_{1/3}Nb_{2/3}O_3$ [2]. Alternatively, there exist lead-free mixed perovskites such as $KTa_{1-x}Nb_xO_3$ (KTN) or $K_{1-x}Li_xTaO_3$ (KLT), which exhibit similar properties, but are much less complicated than the lead relaxors [3,4] and therefore better suited for an investigation into the fundamental origin and mechanism of the relaxor behavior.[2] In KTN and KLT, the single most important feature that can lead to the relaxor behavior is the off-centering of Nb [7] or Li [8–10] and the resulting formation of polar nanoregions. One of us in his previous work have shown that these regions and their capability of reorientational dynamics, are responsible for the first-order Raman scattering [11–15], the unusual softening of the elastic constants, the existence, even in the paraelectric phase, of the dielectric polarization hysteresis loops and their frequency dispersion, the pretransitional diffuse neutron scattering and, finally, for the original coupling between polarization and strain in the relaxor materials. The mechanism of this coupling was the best evidenced in our recent studies of remarkable dielectric resonances observed in KTN and KLT [4–6], as well as in $PbMg_{1/3}Nb_{2/3}O_3$ [4,5]. In the present study, we want to take a new look at the Raman spectra of these systems, in the light of this polarization–strain coupling or, more precisely, of the interaction between acoustic phonons and the orientational motion. This interaction represents a kind of a rotational–translational (R–T) coupling that is common for *any*

* Corresponding author. Fax: +1-610-7585730.
E-mail address: ovs2@lehigh.edu (O. Svitelskiy).
[1] On leave from the Institute of Semiconductor Physics, Kyiv 03650, Ukraine.
[2] Besides alkali perovskites, there are some other mixed crystals, like $SrTiO_3$ doped with Bi, or $BaTiO_3$ doped with Sn, Ce, Zr, etc. that can be used as model relaxors.

0022-3697/03/$ - see front matter © 2003 Elsevier Science Ltd. All rights reserved.
PII: S0022-3697(02)00369-4

system with orientational disorder (including molecular crystals and glasses).

1.1. KTN as a ferroelectric with orientational disorder

The host system, $KTaO_3$, is a highly polarizable paraelectric material, that has a cubic perovskite structure with Ta ions occupying the centers of the cells. It does not undergo any phase transition, but a smallest admixture of either Li or Nb causes one or more. In particular, Nb ions replacing Ta go off-center in a ⟨111⟩ direction, endowing the cell with a permanent electric dipole moment [7]. In the high-temperature phase, these moments are randomly distributed and reorient rapidly among eight equivalent ⟨111⟩ directions so that, on average, the cubic symmetry of the lattice is preserved. With lowering of the temperature, the growing role of the dipole–dipole interactions leads to the formation of precursor clusters (polar nanoregions) characterized by permanent giant electric dipole moments and local distortions from the cubic symmetry [11–15]. If the concentration of Nb is sufficiently high ($x \gtrsim 5\%$) then, when the temperature reaches certain critical values T_{c1}, T_{c2}, T_{c3}, the development of these clusters causes the crystal to undergo a cubic–tetragonal–orthorhombic–rhombohedral (C–T–O–R) sequence of phase transitions. If $0.8 \lesssim x \lesssim 5\%$, the crystal goes from the C phase directly to a R phase. If $x \lesssim 0.8\%$, no transition, but a freezing occurs [16].

In the ideal cubic structure, all zero wavevector phonons are of odd parity, so first-order Raman scattering is forbidden [17] and the spectrum consists only of second-order scattering peaks. However, the structural distortions that accompany the formation of the polar nanoregions break the local cubic symmetry and allow for the appearance and growth (from, approximately $T_{c1} + 20$ K) [11–15] of first-order scattering from the transverse polar optic modes: hard TO_2, TO_4 and soft TO_1. At T_{c1}, the non-polar hard optical mode TO_3 also appears, marking the first structural transition. Throughout this process, the frequencies of the hard modes remain unchanged, but the frequency of the soft mode continuously decreases and reaches a minimum in a vicinity of the phase transition [18–23].

In KTN, the ferroelectric soft mode, a general property of crystals undergoing a displacive phase transition, coexists with a central peak, a common feature of order–disorder phase transitions. Among the several models proposed to explain the central peak [24–28], the most promising one is based on the orientational disorder of Nb-ions moving among eight equivalent sites, offered by Sokoloff [26–28]. While the C phase is characterized by equal probabilities of occupation of all eight sites, phases of lower symmetry restrict the number of equivalent sites that are accessible for a given Nb ion to four neighboring sites in the T phase, to two sites in the O phase and, finally, to a single site in the R phase. The intersite orientational motion is, therefore, a property of the C, T and O phases, albeit increasingly more restricted, but vanishes in the rhombohedral phase. It has a tunneling rather than a hopping character, and gives rise to the Raman central peak. Unfortunately, Sokoloff restricted himself to study of the CP behavior only in a vicinity of the C–T phase transition, so his work is far from being complete.

In the present paper, we show the results of our light scattering study of the interaction of this reorientational motion and acoustic modes. This interaction has so far not been discussed in studies of relaxor ferroelectrics. But, in our view, it lies at the heart of the unusual polarization–strain coupling in relaxors and is central for understanding the relaxor mechanism. The idea of this work originates from earlier studies of softening of elastic constants c_{11} and c_{44} in KTN on approach to the transition, which could not be explained simply by TO–TA mode coupling theory that worked successfully for pure ferroelectrics [29,30]. Especially puzzling was the behavior of the constant c_{11}, since it corresponds to a longitudinal distortion and, therefore, not expected to couple to a transverse optic mode. To resolve this contradiction, one of us proposed [31] that the softening of these constants was caused by the interaction of acoustic phonons with reorienting polar clusters. Their capability to the reorientational dynamics was evidenced by study of the temperature and frequency dependencies of the dielectric hysteresis loops that appear together with the polar nanoregions. The formation of these regions is also accompanied by the appearance and growth of dielectric resonances that are the direct consequences of a coupling between polarization and strain [4–6]. In the same temperature range, the dielectric constant, while still increasing, falls below the values predicted by Curie–Weiss law. Thus, even though the dielectric constant indicates a reduction in softening of the system upon approaching the transition, the polarization–strain coupling increases. Moreover, these resonances continue to be observed below the first transition, i.e. when the soft mode frequency increases. This suggests the continuation of the coupling down to the third (O–R) transition, when rotations stop. Some of the consequences of coexistence of the ferroelectric soft mode with the reorienting polar regions for the dielectric constant of mixed ferroelectrics have received quantitative evaluation in works of Prosandeev et al. [32–34]. It is reasonable to expect that the reorientational motion of these polar nanoregions in the result of a strong polarization–strain coupling will interact and modify the translational motion in crystal and will be observable through the Raman spectra. This motion might also be responsible for disagreement at the zone boundary between measured TA phonon energy and its theoretically predicted value (Fig. 7 in Ref. [22]).

1.2. Comparison with cyanides and Michel's theory

In developing the present interpretation, we have also drawn from the understanding that has been gained through investigations of another type of materials with internal orientational degrees of freedom, namely, alkali–halide–cyanide compounds (like $(KCN)_x(KBr)_{1-x}$ or $(KCN)_x$ $(KCl)_{1-x}$, etc.). In their high-temperature phase, these compounds have an fcc cubic structure (rocksalt) in which the CN^- molecules occupy halogen sites and rapidly reorient among equivalent ⟨111⟩ directions [35]. For sufficiently high CN^- concentrations, lowering temperature causes a transition to either an orthorhombic or a monoclinic phase (depending on x), with the CN^- molecules oriented along one of the ⟨110⟩ directions of the cubic phase [36–38]. Most important for our purpose, this transition is accompanied by the softening of the transverse acoustic (TA) mode and, correspondingly, of the c_{44} elastic constant. For low CN^- concentrations, ($x < 0.56$ for $(KCN)_x(KBr)_{1-x}$ or $x < 0.8$ in $(KCN)_x(KCl)_{1-x}$), the crystal does not undergo any transition, but upon lowering temperature, exhibits a freezing of the dipole orientations [35,39,40]. In both concentration regimes, the TA mode frequency reaches a minimum at the temperature below which the rotations cease, i.e. at the phase transition or freezing temperature. Yet, it is essential to note that these alkali–halide–cyanide compounds do not exhibit a soft optic mode as does KTN.

The alkali–halide–cyanide system is similar to KTN in that, in the high-temperature phase, both types of compounds possess an average cubic symmetry characterized by orientational dynamical disorder. As the temperature is lowered and as the crystalline structure changes, this dynamic disorder becomes increasingly more static. Numerous studies have shown that the cyanide system [41] and its Raman spectra [42,43] can be successfully described by the extended Devonshire model of a rotator in a cubic field [44] interacting strongly with translational oscillations. At the transition temperature, this interaction reaches its maximum strength [36,37] and the effective orientational interaction (rotator–rotator), which arises from it, determines the nature of the phase transition [45]. A detailed investigation of the R–T coupling in solids has been carried out by Michel. It explains the appearance of the central peak in neutron and Raman scattering spectra as well as predicts the softening of the transverse acoustic phonon mode upon approaching the transition temperature, thus proving the validity of an order–disorder model for the phase transition in the mixed alkali–halide–cyanides [46–51].

According to Michel's model, the motion of a linear molecular ion in an octahedral environment can be described by a Hamiltonian that takes into account the translational and rotational motion as well as their coupling

$$H = H^{\mathrm{T}} + H^{\mathrm{R}} + H^{\mathrm{TR}}. \tag{1}$$

The translational and rotational part are the usual ones [46–51] and need not be reproduced here. The term responsible for the R–T interaction can be approximated as

$$H^{\mathrm{TR}} = \sum_{\vec{k}} \mathrm{i} Y^{+} \hat{v} s, \tag{2}$$

where $s(\vec{k})$ is the Fourier transformed center of mass displacement of the unit cell and $Y(\vec{k})$ is an eigenvector representing rotations. Its components, Y_α, are linear combinations of spherical harmonics Y_l^m of order two

$$\vec{Y} = \begin{pmatrix} Y_2^0 \\ \sqrt{\frac{3}{2}}(Y_2^2 + Y_2^{-2}) \\ \mathrm{i}(Y_2^2 - Y_2^{-2}) \\ (Y_2^1 - Y_2^{-1}) \\ -\mathrm{i}(Y_2^1 + Y_2^{-1}) \end{pmatrix}. \tag{3}$$

Two of them have E_g and the other three T_{2g} symmetry. The 3×5 matrix $\hat{v}(\vec{k})$ reflects the strength of the coupling and is completely specified in terms of a microscopic octahedral potential. This R–T coupling leads to an effective interaction between rotating molecules whose motion is coupled via the acoustic phonons

$$V_{\mathrm{eff}} \sim \sum_{\vec{k}} Y^{+} \hat{C} Y, \tag{4}$$

where $C(\vec{k}) = v^{\mathrm{T}} M^{-1} v$ and M is the coupling matrix determined by the harmonic part of the translational potential. This interaction is an addition to the single particle Devonshire potential V^0.

Michel used the above Hamiltonian (1) to calculate the elastic constants c_{44} and c_{11} and found

$$\begin{aligned} c_{44} &= c_{44}^0(1 - R_{44}\delta/T) \qquad \text{and} \\ c_{11} &= c_{11}^0(1 - R_{11}\gamma/T), \end{aligned} \tag{5}$$

where c_{44}^0 and c_{11}^0 are the elastic constants in the absence of coupling; δ and γ are the eigenvalues of the effective interaction, V_{eff}. R_{44} and R_{11} with T_{2g} and E_g symmetries are defined by a single particle orientational susceptibility $\hat{R}$

$$R_{\alpha\beta} = \frac{\mathrm{Tr}(\mathrm{e}^{-V_0/T} Y_\alpha^{+} Y_\beta)}{\mathrm{Tr}(\mathrm{e}^{-V_0/T})}. \tag{6}$$

The trace Tr stands for integration over the solid angle. Because $\omega_1^2 = \omega_2^2 \propto c_{44}$ and $\omega_3^2 \propto c_{11}$, the frequencies of the corresponding modes can be written as

$$\begin{aligned} \omega_1^2 &= \omega_2^2 = \Omega_1^2(1 - y\delta/T) \qquad \text{and} \\ \omega_3^2 &= \Omega_3^2(1 - x\gamma/T). \end{aligned} \tag{7}$$

Here, Ω_1 and Ω_3 denote the mode frequencies in the absence of coupling.

Michel's model has been successfully tested, mainly, on the alkali–halide–cyanide compounds using various experiments: absorption and scattering of light [40–43],

neutron scattering [37–39,45], elastic constant measurements [52]. In all cases, it has been found to be in good agreement with experimental data. In particular, the elastic constants have been found to decrease with temperature down to the transition, in agreement with Eq. (5).

As we said, in KTN, a softening of the TA phonon [53,30] as well as a decrease in the elastic constants c_{11} and c_{44} [31] has also been observed. In pure or simple ferroelectrics, a softening of the TA mode (and corresponding elastic constant c_{44}) has been explained in terms of an interaction between the TA and the soft TO ferroelectric mode [29,30]. However, as our data indicate, in mixed ferroelectrics, the formation of polar nanoregions with orientational degrees of freedom and the local distortions and strain fields associated with them, can alter the role of the classical soft-mode mechanism in the transition. We already mentioned the unexpectedness of softening of the elastic constant c_{11} for classical TO–TA mode coupling model. Presented here results show difficulties of this approach explaining softening of the TA phonon, especially, below the first transition temperature. On the other hand, we demonstrate that these contradictions might be resolved by taking into consideration the orientational dynamics of the polar regions and its coupling to the TA phonon modes. To make this explanation, we have to utilize the approach developed by Michel for the disordered crystals, which do possess orientational dynamics, do not possess a soft optic mode, yet still exhibit softening of their transverse acoustic mode.

2. Experiment and results

We have studied the temperature dependence of polarized $\langle y|zz|x\rangle$ (VV) and depolarized $\langle y|zy|x\rangle$ (VH) Raman scattering spectra of several $\langle 100\rangle$-cut $KTa_{1-x}Nb_xO_3$ samples. However, in this paper, we concentrate primarily on the most characteristic results, which were obtained on a sample containing 15% of Nb. The scattering was excited by 514.5 nm light from a 200 mW Ar^+-ion laser, focused to a 0.1 mm spot. The scattered light was collected at an angle of 90° with respect to the incident beam by a double-grating ISA Jobin Yvon spectrometer equipped with a Hamamatsu photomultiplier R-649. For most of the measurements, the slits were opened to 1.7 cm^{-1}. However, in order to acquire more precise data in the central peak region, the slits were narrowed to 0.5 cm^{-1}. Both polarizations of the scattered light, VV and VH, were measured separately. In order to exclude differences in sensitivity of the monochromator to different polarizations of the light, a circular polarizer was used in front of the entrance slit. To protect the photomultiplier from the strong Rayleigh scattering, the spectral region from -4 to $+4$ cm^{-1} was excluded from the scans. The data were collected in several cooling–warming cycles. In each cycle, the sample was cooled from room temperature down to 80 K and then warmed up, at an average rate of 0.2–0.4 K/min, in temperature steps of 5–10 K. At each step, the temperature was stabilized and the Raman spectra measured. Cooling and warming cycles were performed without application of electric field as well as with a 1.2 kV/cm electric field applied in the z direction, perpendicular to the scattering plane. Below 150 K, the Raman spectra revealed thermal hysteresis effects. For the sake of clarity, we concentrate on data measured upon cooling, unless specified otherwise. Both, neutron scattering [54] and our data indicated phase transitions at the following temperatures: $T_{c1} \approx 135$ K, $T_{c2} \approx 125$ K and $T_{c3} \approx 110$ K. Starting at approximately T_{c1}, the sample becomes milky. Near T_{c3} the milkiness suddenly grows to such a degree that all polarization information is lost.

Raman spectra with polarization analysis of the scattered beam were measured as a function of temperature. Fig. 1 shows examples of the VV (a) and VH (b) spectra at four temperatures: 200, 140, 130 and 120 K. Due to its low intensity, the VH component has been magnified by a factor of eight. Upon lowering the temperature, the first-order lines (TO_1, TO_2, TO_3, TO_4) appear on top of a strong and broad second-order spectrum of which the 2TA is the most intense feature. For details in line assignment, see Refs. [21,22,55,56]. Here, we focus our attention primarily on the second-order spectrum and its evolution with temperature. With decreasing temperature, and transitions to phases of lower symmetries that restrict reorientational freedom of Nb ions, the VH component of the second-order spectrum can be seen to decrease dramatically, while its VV counterpart remains relatively unchanged. The reported decrease is first noticeable at 140 K and continues until the VH component of the second-order scattering is hardly visible, below 120 K. Therefore, this intensity decrease correlates with the appearance of the polar phase. Unfortunately, we were unable to track this effect below the third phase transition temperature, T_{c3}, because the polarization information was lost due to increasing milkiness of the sample.

Concurrently to the vanishing intensity of the VH component of the 2TA peak, its frequency can also be seen, in Fig. 2, to decrease progressively and reach a minimum at T_{c3}. It is worth noting that the curve is relatively smooth, and that the two higher transitions produce only slight inflections in the curve, if at all.

Changes in the rotational freedom of Nb ions are also reflected in the central peak. Though the central part of the spectrum from -4 to $+4$ cm^{-1} was cut off, the central peak was found to exceed this range sufficiently so that it could be fitted adequately and its magnitude and width determined. The fitting function used was Lorentzian. Fig. 3 shows plots of the amplitude (a) and FWHM (b) obtained from the fits of both VV (solid triangles) and VH (open triangles) components. An insert illustrates the quality of our Lorentzian approximation. As seen from Fig. 3, in the high-temperature limit (cubic phase), the central peak is dominated by the VV component. With lowering temperature, the growth of

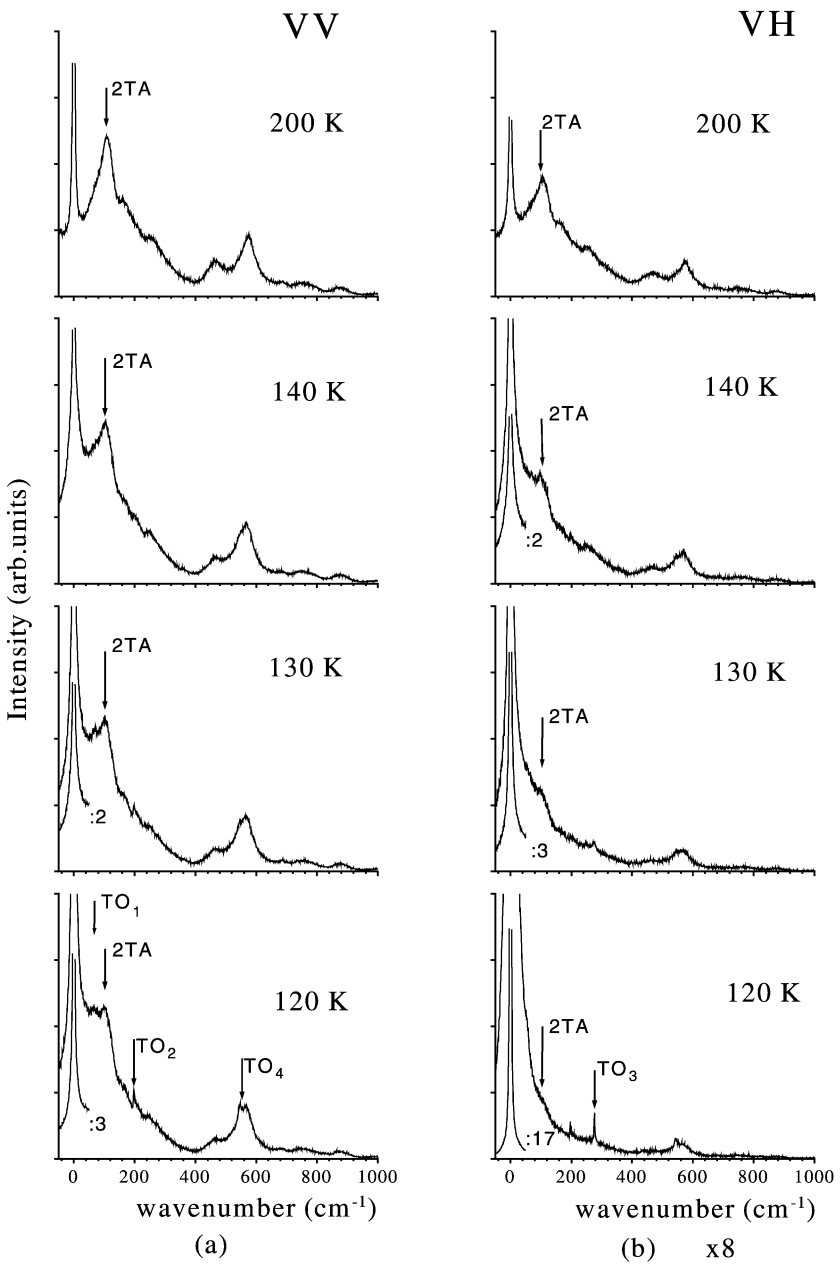

Fig. 1. VV (a) and VH (b) components of the Raman spectra at different temperatures.

the dynamical precursor polar clusters, at approximately $T \approx 155$ K ($T_{c1} + 20$ K), is marked by a decrease of the VV intensity and a broadening of the central peak in both VV and VH geometries. With further development of the polar clusters, the central peak intensity grows and its width decreases. On approach to T_{c3}, the intensity reaches a maximum and the width, a minimum. The intensity maximum in VH is even higher than in VV geometry. After the transition to the R phase, Nb ions become 'locked in' (or confined to) only one site and the central peak disappears. Comparing with Fig. 2, one can see that the cessation of the reorientational motion changes temperature behavior of the frequency of the TA phonon.

To get a deeper insight in the processes, we repeated the same set of measurements in the presence of the electric bias field. Fig. 4 presents a comparative plot where we show examples of data taken at temperatures 150 K (a) and 130 K (b) without field and with a 1.2 kV/cm field applied in a direction perpendicular to the scattering plane. For a more complete comparison, we show not only the data

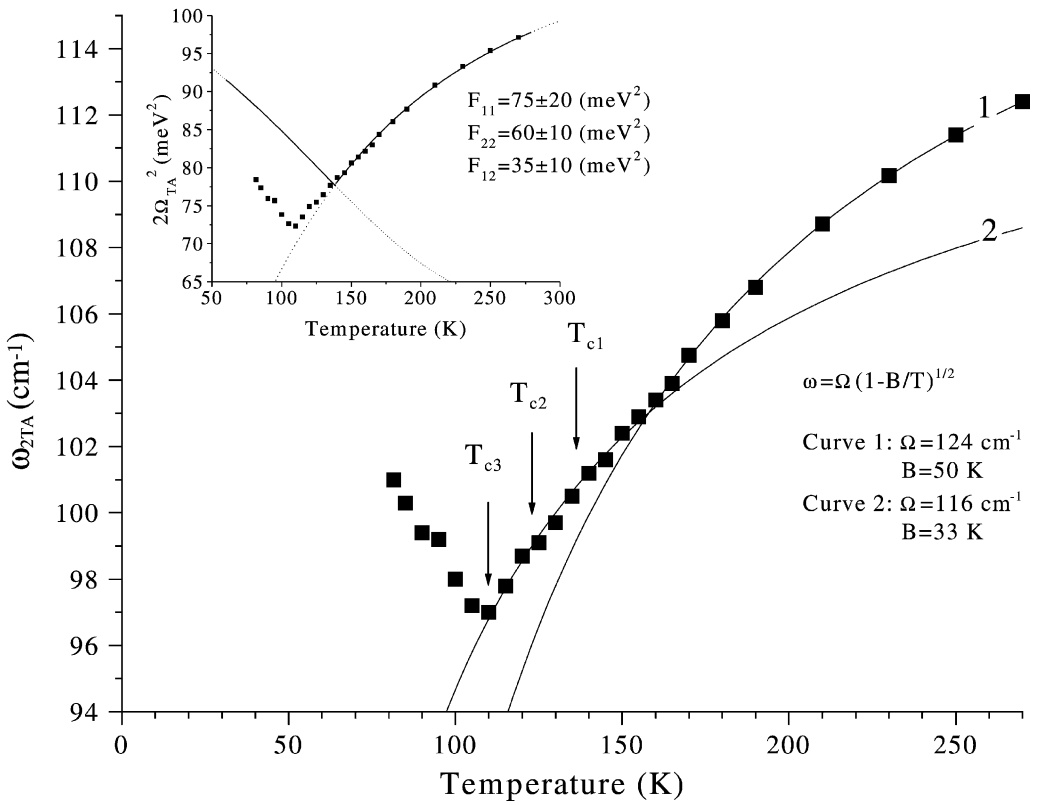

Fig. 2. Softening of the 2TA mode on the approach to the temperature of the third phase transition. Squares show experimental data, solid lines, results of fit based on rotational–translational coupling theory. Appearance of the polar clusters changes the character of coupling and modifies the parameters of the fitting curve. Insert shows the best-fit results based on traditional TO–TA mode coupling theory (values of parameters are outside the expected range).

taken upon cooling, but also the data taken upon warming the sample up from 80 K. This plot reveals another effect that we are the first to observe. In both cooling and warming cycles, application of an electric field causes an increase in the depolarized and a decrease in the polarized intensity of the second-order spectra (lines 1 and 3 to be compared to lines 2 and 4, respectively). The effect of the field is stronger upon warming, i.e. after the sample has been cooled to 80 K, well into the more ordered rhombohedral phase.

In Section 3, we present an interpretation that consistently explains all the phenomena described above

(i) the intensity decrease of the depolarized second-order scattering after transition to the low-symmetry phases upon zero-field cooling;
(ii) the softening of the zone boundary TA mode (seen in Raman spectrum as 2TA peak) on approach to the phase transition temperature;
(iii) the central peak evolution in the temperature region of phase transitions;
(iv) the field-induced intensity changes in the scattered light.

3. Analysis and discussion

The first experimental observation is that the decrease in intensity of the second-order depolarized spectrum, visible in Fig. 1, closely correlates with the formation and development of polar clusters. The latter formation is evidenced by the appearance and growth in the spectrum of first-order scattering peaks due to the polar optic modes, TO_2, TO_3, TO_4 and TO_1. These modes, forbidden by symmetry in the cubic phase, necessarily signal symmetry breaking at the local level, in this case a tetragonal distortion [11–15]. With the formation of polar clusters, new collective degrees of freedom appear, which correspond to the six possible orientations of the tetragon. Motion between these various orientations affects the off-diagonal components of the polarizability tensor and, therefore, influences the VH scattering. The progressive decrease in intensity of the depolarized components of second-order peaks is consistent with increasing restrictions imposed on the reorientations of the ions within polar clusters by the successive phase transitions: from four in the T phase to two in the O phase and, finally, one in the R phase.

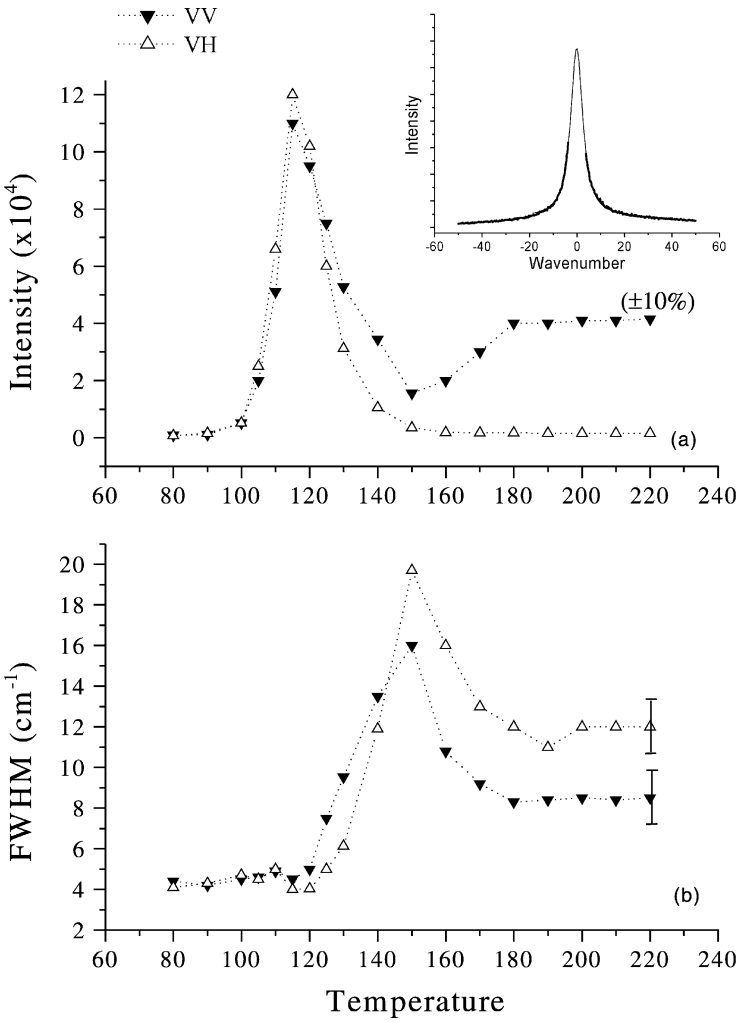

Fig. 3. Temperature dependence of the intensity and width of the central peak, approximated by Lorentzian function (example of approximation is shown on insert).

The second experimental observation of importance is the softening of the transverse acoustic mode (Fig. 2). This softening is consistent with the slowing reorientational dynamics, strengthened by the nucleation of the polar clusters. These polar clusters, with their local strain fields, can especially effectively interact with the acoustic mode and contribute to the decrease of its frequency. By symmetry, T_g rotations couple mostly to the transverse acoustic mode that corresponds to the c_{44} elastic constant (Eqs. (5) and (6)). According to Michel's concept the softening of the acoustic mode is described by Eq. (7). For our purposes we rewrite it as

$$\omega = \Omega\sqrt{(1 - B/T)},$$

where $B = y\delta$ and Ω designates the pure 2TA frequency, uncoupled to rotations. The parameter B is, in general, temperature dependent, but for short temperature intervals, this dependence may be neglected [48,49]. In that case, it has the meaning of a cross-over temperature at which the rotational frequency falls below the frequency of the acoustic mode. In KTN, as in $(KCN)_x(KBr)_{1-x}$ for large x, this cross-over is never reached because a phase transition causes structural changes in the crystal. The result of the fit is shown in Fig. 2 with two solid lines. The first line corresponds to the case of cubic phase. The second line reflects structural changes that develop in the crystal due to the evolution of the polar phase. It is important to note that, although the experimental curve does not display any remarkable changes at the phase transition temperatures, it does show a 'reduction' in softening of the TA mode with the growth of the polar distortions. This reduction indicates that the distorted lattice has new values of the involved parameters, B and Ω. It is reasonable to suppose that the adjustment of

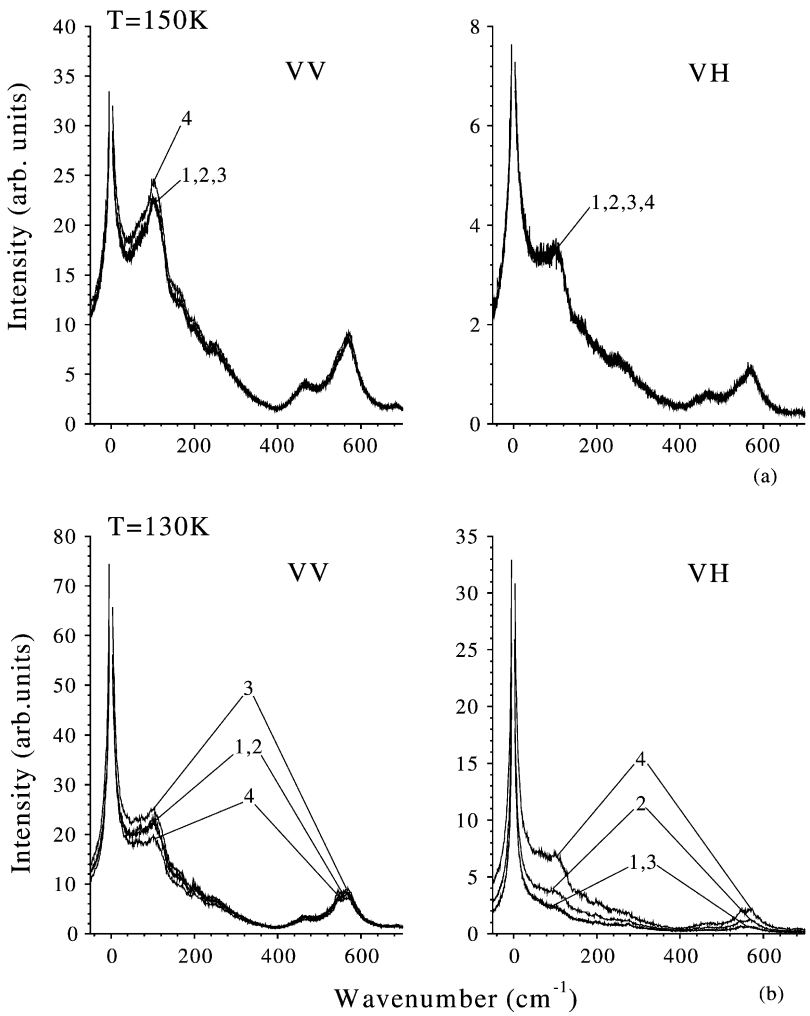

Fig. 4. An illustration of the influence of electric field measured both, upon cooling and warming, on the polarized and depolarized Raman scattering at 150 K (a) and 130 K (b). Line 1 is measured upon zero field cooling, line 2 upon cooling with 1.2 kV/cm electric field. Line 3 is measured upon zero field warming, line 4 upon warming with 1.2 kV/cm electric field.

these parameters actually occurs in steps, so at each phase transition they obtain new values. However, the resolution of our experiment is not sufficient to observe these details.

For comparison and for completeness of the picture, we also made an attempt to approximate this curve by the traditional TO–TA mode coupling approach, following Axe's work [29]. To estimate the temperature dependence of the soft ferroelectric TO_1 mode we used an approximation of the actual data measured on the sample containing 15.7% of Nb [57]. It is remarkable, that according to these measurements, the TO_1 mode has its minimum at a temperature approximately 5 K higher than T_{c1}. (Similar measurements on a 1.2% KTN crystal also showed such a temperature difference 5 K [11,58,59]). This fact allowed us to make an adjustment to our value of T_{c1}. Consequently, we wrote TO_1 frequency as

$$\Omega_{TO_1} = \begin{cases} \sqrt{24(\pm 5) + 0.47(\pm 0.05)(T - 140(\pm 5))}, & T > 140\ \mathrm{K} \\ 11(\pm 1) - 0.038(\pm 0.003)T, & T < 140\ \mathrm{K} \end{cases}.$$

Axe's parameters F_{11}, F_{22}, F_{12} were treated as free. The result of the fit and the best-fit values of the parameters are shown in the insert to Fig. 2. The first thing that strikes the eye is the continuation of the TA mode softening till much lower temperatures then expected from the classical mode coupling theory. It is important to note, that while the values of F_{11} and F_{22} do agree within the error bars to those, predicted by Axe, the value of the parameter F_{12} (which corresponds to the cross-term, responsible for coupling) is

significantly higher than the one expected by Axe at the zone boundary. This fact reflects insufficiency of the TO–TA mode coupling theory to explain the acoustic mode softening even at temperatures above 140 K. Consequently, taking in to account the effect of the reorientational–translational coupling is necessary for providing an explanation for the softening of the TA mode and can constitute a challenging problem for a theoretical physicist.

According to Refs. [46–51], slowing down of the rotations should also lead to the growth of the central peak, which is a common property of systems with slow relaxations. In the present case, the central peak can be understood in the frame of the modified eight site model, based on the one described by Sokoloff [26–28]. As we explained above, lowering of the temperature leads to appearance of the polar clusters, transitions to lower symmetry phases, restrictions on the number of allowed sites and growing correlations between Nb ions. As a result, at high temperature (Fig. 3), a significant contribution of 180° reorientations to the scattering process (which, by symmetry, do not contribute to VH scattering) causes the dominance of the VV component of the central peak over the VH one. Restriction of these 180° reorientations, caused by the nucleation of the polar clusters, leads to a decrease in intensity of the VV component and to a corresponding increase in the intensity of the VH one. Concurrently, their widths increase and reach maxima on approach to the first transition at T_{c1}. Below this temperature, in the tetragonal phase where the sample is divided into ferroelectric domains, growing correlations between Nb ions lead to an increase in relaxation time and to the narrowing and growth of both VV and VH components of the central peak. This process continues through the second transition at T_{c2} in the O phase. It is remarkable that the VH component grows faster and becomes even more intense than the VV. Its intensity reaches a maximum and width a minimum on approach to the third transition temperature $T_{c3} \approx 110$ K. In the rhombohedral phase, the Nb ions can no longer reorient and the central peak disappears.

This reorientational dynamics coexists with the ferroelectric soft mode TO_1. The peculiarity of this mode in KTN is that it softens only partially, going through a relatively high energy minimum close to the first transition. Consequently, only the motion of individual Nb ions is able to follow the soft phonon dynamics. At the same time, the reorientational motion of the polar clusters, since it occurs at much lower frequency, can influence the transverse acoustic phonons frequencies and give rise to the central peak. Thus, two types of reorientational relaxations are expected to coexist: (i) the fast relaxation of individual Nb ions, both within clusters and outside of them, and (ii) the slow relaxation of the entire cluster, i.e. the cooperative relaxations of all the Nb ions within the cluster (Fig. 5). It looks that, in each phase, precursor clusters of the lower-symmetry phase are present. Therefore, in the cubic phase (Fig. 5a), the two time scales can appear (i) from the reorientation of Nb ions among equivalent orientations relative to the polar axis of the precursor cluster and (ii) from the reorientation of the precursor cluster as a whole relative to the crystal axes. Once the rotation of the cluster is 'locked' in the T phase (Fig. 5b), a precursor distortion leading to the next, orthorhombic, phase appears. In other words, among four allowed sites, two become preferred, thus forming a cluster with monoclinic distortion and two possible orientations. Again, (i) the fast relaxation originates from the motion between equivalent sites within the same direction of monoclinic distortion and (ii) the slow relaxation appears due to the reorientational motion between the two possible monoclinic axes (between different pairs of equivalent sites).

The observed effect of a bias electric field (Fig. 4) confirms the above interpretation. A field introduces preferred direction in space, along which the Nb ions and polar regions will tend to orient. In our case, the field was applied in the z direction, orthogonal to the scattering plane $x - y$ (Fig. 5b). As a result, Nb ions became constrained to move only in this plane, e.g. amongst four equivalent positions. Such a motion, in the tetragonal and orthorhombic phases, enhances the depolarized scattering while preventing the polarized one. This effect is clearly seen in Fig. 4, where one should compare the lines 1 and 2 (upon cooling) or the lines 3 and 4 (upon warming), noticing that the effect of the field is further enhanced by thermal hysteresis.

One of the consequences of our model is the following: a depolarized component of second-order Raman scattering exists, primarily, due to the coupling of transverse acoustic modes to the reorientational motion of Nb ions within polar clusters. To verify this statement, we have measured samples with low (1.2%) and high (40%) concentrations of Nb. In the first case, at sufficiently high temperature, each Nb ion can be considered as an approximately free rotator undergoing fast relaxation. It can be shown [60], that the depolarization ratio I_{VH}/I_{VV} (I_{VH} and I_{VV} are the intensities of the depolarized and polarized light scattering) for a system of free rotators in isotropic space is equal to 0.75. Consequently, if such a coupling indeed takes place, we expect to find a depolarization ratio of 0.75 for the second-order peaks too. Lowering the temperature should result in a decrease of I_{VH}/I_{VV}. The experiment did show that this ratio decreases from 0.75 at room temperature to 0.55 (± 0.05) at the temperature of transition at ~ 15 K. In the second case, the interaction between the neighboring Nb ions is strong even in the high-temperature phase; so they cannot be considered as free rotators at all. Therefore, the VH component of scattering will be small and the depolarization ratio should go to zero. Measurements of the 40% sample yielded a value of the ratio of 0.04 (which is on the level of the experimental error).

We have demonstrated the importance of the reorientational motion of Nb ions as it slows down and the polar clusters form. Various effects, related to their formation, become apparent at different temperatures. Since the

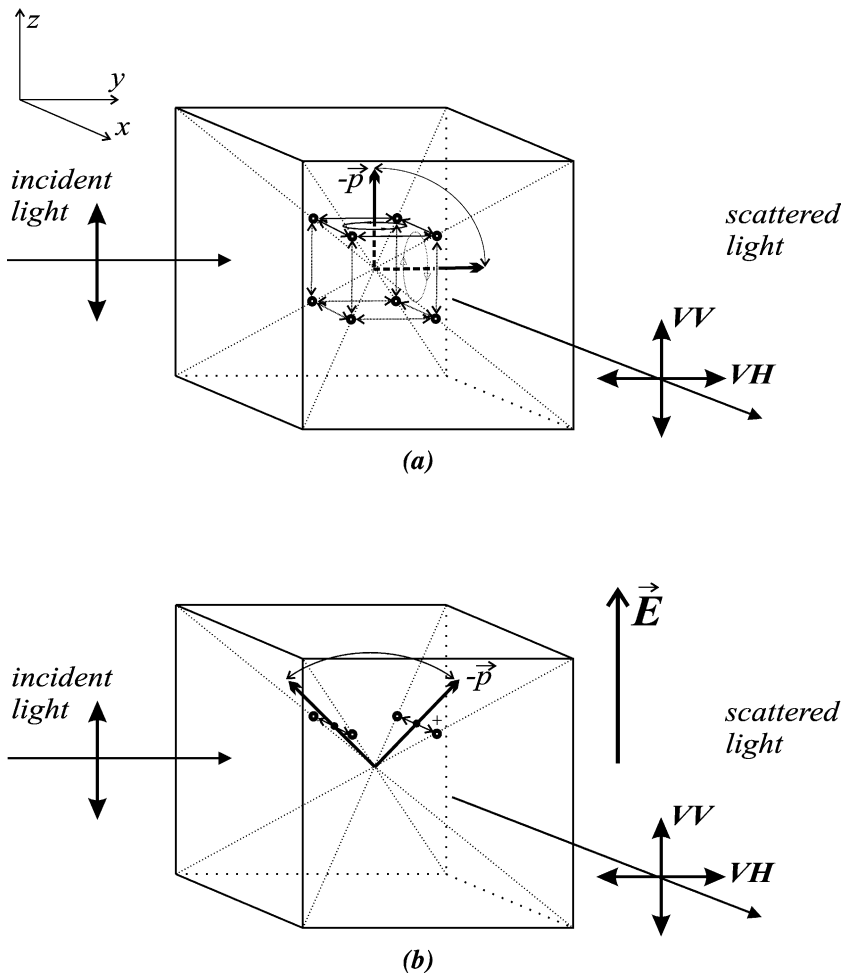

Fig. 5. Two relaxation time scales: (a) in a precursor polar cluster in the cubic phase there is a fast motion in (100) plain and slow—among different planes; (b) in the cluster, locked by an external field, a monoclinic distortion becomes important; motion is fast along [100] side and slow—among different sides.

relaxor behavior is inseparably related to the presence of the polar clusters, we would like to stop on the question of their development. In the lead relaxors, the temperature of the formation of the polar clusters is often referred to as Burns temperature T_d and located several hundred degrees above the temperature of the maximum of the dielectric constant [61,62]. One of the effects marking T_d, is the deviation of the dielectric constant from Curie–Weiss law [63]. In one of the previous works [64], we have shown that in KTN such a deviation occurs approximately at a temperature $T_c + 20$ K. However, the softening of the TA phonon (Fig. 2) and the temperature evolution of the central peak (Fig. 3) suggest that the nucleation of the lattice distortions starts at much higher temperatures. A direct confirmation of this suggestion can be found from consideration of the first-order peaks. The most apparent example is given in Ref. [15] (Fig. 1a), which shows signs of the presence of a broad reminisce of the TO_2 peak up to 150° above T_c. Since in the cubic symmetry this peak is prohibited by selection rules, we have to assume that the distorted regions are present even at this high temperature. The lifetime of these regions must be too short for their detection in the dielectric constant measurements. With lowering temperature, the lifetime of the distortions increases. At a temperature of $T_c + 20$ K, the polar clusters become sufficiently stable to cause the deviation of the dielectric constant from Curie–Weiss law. The relation between the appearance of the polar clusters and the Burns temperature demonstrates the difference between KTN and lead compounds and establishes a limit of using KTN as a model system for lead relaxors.

Our results indicate that the depolarized second-order scattering is a sensitive probe for the reorientational motion of both, Nb ions and polar nanoregions. Analogy to other types of orientationally disordered systems shows that the rotational–translational coupling is an important

and universal feature of the dynamics of disordered systems. It has been evidenced and studied in molecular crystals and it may also contribute to an explanation of the Boson peak observed in the Raman spectra of glassy materials [65], which represent a case of complete disorder. Even though the origin of the Boson peak is still not known, it has been found to be a universal property of the glassy state and, as we show here, signs of it are also apparent in disordered crystals. Its origin cannot be explained simply by acoustic phonons, but appears to contain a significant contribution from localized modes [65]. In glass forming liquids, such as salol, the depolarized light scattering has been shown to be due to fluctuations in molecular orientations [66]. We suggest here that there must be a similar contribution of orientational fluctuations to Raman scattering in disordered crystals and provide experimental evidence in support of this claim in the case of $KTa_{1-x}Nb_xO_3$.

4. Conclusion

The results presented here show the essential role played by orientational motion in disordered ferroelectric KTN crystals. As in cyanide compounds, it couples strongly to the translational oscillations and also gives rise to the central peak. This conclusion, together with earlier results obtained on glassy materials, shows the fundamental nature of such a coupling and suggests in return that the Boson peak in glasses may also be due to coupling between rotational and translational oscillations.

Acknowledgements

We are grateful to L.A. Boatner for the KTN crystals and to G. Yong for helpful discussions. This work was supported by a grant from NSF No. DE-FG02-00ER45842.

References

[1] I.G. Siny, S.G. Lushnikov, R.S. Katiar, V.H. Schmidt, Ferroelectrics 226 (1999) 191.
[2] A. Lebon, M. El Marssi, R. Farhi, H. Dammak, G. Calvarin, J. Appl. Phys. 89 (2001) 3947.
[3] G. Yong, J. Toulouse, R. Erwin, S.M. Shapiro, B. Hennion, Phys. Rev. B 62 (2000) 14736.
[4] J. Toulouse, R. Pattnaik, J. Korean Phys. Soc. 32 (1998) S942.
[5] R. Pattnaik, J. Toulouse, Phys. Rev. Lett. 79 (1997) 4677.
[6] J. Toulouse, R. Pattnaik, Phys. Rev. B 65 (2001) 024107.
[7] O. Hanske-Petitpierre, Y. Yakoby, J. Mustre De Leon, E.A. Stern, J.J. Rehr, Phys. Rev. B 44 (1991) 6700.
[8] J.J. Van der Klink, D. Rytz, F. Borsa, U.T. Höchli, Phys. Rev. B 27 (1983) 89.
[9] E.A. Zhurova, V.E. Zavodnik, S.A. Ivanov, P.P. Syrnikov, V.G. Tsirelson, Z. Naturforsch 48 (1993) 25.
[10] E.A. Zhurova, V.E. Zavodnik, S.A. Ivanov, P.P. Syrnikov, V.G. Tsirelson, Russ. J. Inorg. Chem. 37 (1992) 1240.
[11] J. Toulouse, P. DiAntonio, B.E. Vugmeister, X.M. Wang, L.A. Knauss, Phys. Rev. Lett. 68 (1992) 232.
[12] J. Toulouse, R.K. Pattnaik, J. Phys. Chem. Solids 57 (1996) 1473.
[13] P. DiAntonio, B. Vugmeister, J. Toulouse, L.A. Boatner, Phys. Rev. B 47 (1993) 5629.
[14] E. Bouziane, M.D. Fontana, J. Phys. Chem. Solids 57 (1996) 1473.
[15] P. DiAntonio, J. Toulouse, B.E. Vugmeister, S. Pilzer, Ferroelectr. Lett. 17 (1994) 115.
[16] D. Rytz, H.J. Scheel, J. Cryst. Growth 59 (1982) 468.
[17] P.A. Fleury, J.M. Worlock, Phys. Rev. 174 (1968) 613.
[18] H. Uwe, K.B. Lyons, H.L. Karter, P.A. Fleury, Phys. Rev. B 33 (1986) 6436.
[19] T.G. Davis, J. Phys. Soc. Jpn 28 (1970) 245.
[20] G.E. Kugel, M.D. Fontana, Ferroelectrics 120 (1991) 89.
[21] G.E. Kugel, H. Mesli, M.D. Fontana, D. Rytz, Phys. Rev. B 37 (1998) 5619.
[22] G.E. Kugel, M.D. Fontana, W. Kress, Phys. Rev. B 35 (1987) 813.
[23] R. Migoni, H. Bilz, D. Bäuerle, Phys. Rev. Lett. 37 (1976) 1155.
[24] E. Lee, L.L. Chase, L.A. Boatner, Phys. Rev. B 31 (1985) 1438.
[25] K.B. Lyons, P.A. Fleury, D. Rytz, Phys. Rev. Lett. 57 (1986) 2207.
[26] J.P. Sokoloff, L.A. Chase, L.A. Boatner, Phys. Rev. B 41 (1990) 2398.
[27] J.P. Sokoloff, L.A. Chase, D. Rytz, Phys. Rev. B 38 (1988) 597.
[28] J.P. Sokoloff, L.A. Chase, D. Rytz, Phys. Rev. B 40 (1989) 788.
[29] J.D. Axe, J. Harada, G. Shirane, Phys. Rev. B 1 (1970) 1227.
[30] R.L. Prater, L.L. Chase, L.A. Boatner, Phys. Rev. B 23 (1981) 221.
[31] L.A. Knauss, X.M. Wang, J. Toulouse, Phys. Rev. B 52 (1995) 13261.
[32] S. Prosandeev, V. Trepakov, S. Kapphan, M. Savinov, B. Burton, E. Cockayne, AIP Proceedings, Fundamental Physics of Ferroelectrics, Williamsburg, 2002.
[33] S.A. Prosandeev, V.A. Trepakov, J. Exp. Theor. Phys. 94 (2002) 419.
[34] S.A. Prosandeev, V.A. Trepakov, M.E. Savinov, L. Jastrabik, S.E. Kapphan, J. Phys.: Condens. Matter 13 (2001) 9749.
[35] K. Knorr, A. Loidl, Phys. Rev. B 31 (1985) 5387.
[36] J.M. Rowe, J.J. Rush, N.J. Chesser, K.H. Michel, J. Naudts, Phys. Rev. Lett. 40 (1978) 455.
[37] J.M. Rowe, J.J. Rush, D.C. Hinks, S. Susman, Phys. Rev. Lett. 43 (1979) 1158.
[38] J.M. Rowe, J.J. Rush, E. Prince, J. Chem. Phys. 66 (1977) 5147.
[39] J.M. Rowe, J.J. Rush, S. Susman, Phys. Rev. B 28 (1983) 3506.
[40] F. Luty, in: V.M. Tuchkevich, K.K. Shvarts (Eds.), Defects in Insulating Crystals, Zinatne Publishing House, Riga, 1981, p. 70.
[41] F. Luty, Phys. Rev. B 10 (1974) 3677.
[42] D. Durand, F. Luty, Phys. Status Solidi B 81 (1977) 443.

[43] D. Durand, F. Luty, Ferroelectrics 16 (1977) 205.
[44] H.U. Beyeler, Phys. Rev. B 10 (1974) 2614.
[45] A. Loidl, F.R. Feile, K. Knorr, B. Renker, J. Daubert, D. Durand, J. Suck, Z. Phys. B 38 (1980) 253.
[46] K.H. Michel, Z. Phys. B 61 (1985) 45.
[47] K.H. Michel, J. Naudts, B. De Raedt, Phys. Rev. B 18 (1978) 648.
[48] K.H. Michel, J. Naudts, J. Chem. Phys. 67 (1977) 547.
[49] K.H. Michel, J. Naudts, Phys. Rev. Lett. 39 (1977) 212.
[50] K.H. Michel, J. Naudts, J. Chem. Phys. 68 (1978) 216.
[51] K.H. Michel, J. Chem. Phys. 84 (1986) 3451.
[52] J.F. Berret, A. Farkadi, M. Boissier, J. Pelous, Phys. Rev. B 39 (1989) 13451.
[53] P.M. Gehring, H. Chou, S. Shapiro, J. Hriljac, D. Chen, J. Toulouse, D. Rytz, L.A. Boatner, Ferroelectrics 150 (1993) 47.
[54] G. Yong, private communication.
[55] W.G. Nielsen, J.G. Skinner, J. Chem. Phys. 47 (1967) 1413.
[56] S.K. Manlief, H.Y. Fan, Phys. Rev. B 5 (1972) 4046.
[57] J. Toulouse, R. Pattnaik, Ferroelectrics 199 (1997) 287.
[58] P.M. Gehring, H. Chou, S.M. Shapiro, J.A. Hriljac, D.H. Chen, J. Toulouse, D. Rytz, L.A. Boatner, Phys. Rev. B 46 (1992) 5116.
[59] H. Chou, S.M. Shapiro, K.B. Lyons, J. Kjems, D. Rytz, Phys. Rev. B 41 (1990) 7231.
[60] D.A. Long, Raman Spectroscopy, McGraw-Hill, New York, 1977.
[61] G. Burns, F.H. Dacol, Solid State Commun. 48 (1983) 853.
[62] G. Burns, F.H. Dacol, Phys. Rev. B. 28 (1983) 2527.
[63] D. Viehland, S. Jang, L.E. Cross, M. Wuttig, Phys. Rev. B. 46 (1992) 8003.
[64] L.A. Knauss, R. Pattnaik, J. Toulouse, Phys. Rev. B 55 (1997) 3472.
[65] C. McIntosh, J. Toulouse, P. Tick, J. Non-Cryst. Solids 222 (1997) 335.
[66] H.Z. Cummins, G. Li, W. Du, R.M. Pick, C. Dreyfus, Phys. Rev. E 53 (1996) 896.